Published in final edited form as:

Cancer Res. 2013 November 01; 73(21): 6516–6525. doi:10.1158/0008-5472.CAN-13-0967.

TIG1 Promotes the Development and Progression of Inflammatory Breast Cancer through Activation of Axl Kinase

Xiaoping Wang[1,2], **Hitomi Saso**[1,2], **Takayuki Iwamoto**[1], **Weiya Xia**[3], **Yun Gong**[2,4], **Lajos Pusztai**[1], **Wendy A. Woodward**[2,5], **James M. Reuben**[2,6], **Steven L. Warner**[7], **David J. Bearss**[7], **Gabriel N. Hortobagyi**[1], **Mien-Chie Hung**[3], and **Naoto T. Ueno**[1,2]

[1]Department of Breast Medical Oncology, The University of Texas MD Anderson Cancer Center, Houston, Texas

[2]Morgan Welch Inflammatory Breast Cancer Research Program and Clinic, The University of Texas MD Anderson Cancer Center, Houston, Texas

[3]Department of Molecular and Cellular Oncology, The University of Texas MD Anderson Cancer Center, Houston, Texas

[4]Department of Pathology, The University of Texas MD Anderson Cancer Center, Houston, Texas

[5]Department of Radiation Oncology, The University of Texas MD Anderson Cancer Center, Houston, Texas

[6]Department of Hematopathology, The University of Texas MD Anderson Cancer Center, Houston, Texas

[7]Tolero Pharmaceuticals, Inc., Salt Lake City, Utah

Abstract

Inflammatory breast cancer (IBC) is the most lethal form of breast cancer, but the basis for its aggressive properties are not fully understood. In this study, we report that high tumoral expression of TIG1 (RARRES1), a functionally undefined membrane protein, confers shorter survival in IBC patients. TIG1 depletion decreased IBC cell proliferation, migration and invasion in vitro and inhibited tumor growth of IBC cells in vivo. We identified the receptor tyrosine kinase Axl as a TIG1 binding protein. TIG1 interaction stablilized Axl by inhibiting its proteasome-dependent degradation. TIG1-depleted IBC cells exhibited reduced Axl expression, inactivation of NF-κB and downregulation of MMP-9, indicating that TIG1 regulates invasion of IBC cells by supporting the Axl signaling pathway in IBC cells. Consistent with these results, treatment of IBC cells with the Axl inhibitor SGI-7079 decreased their malignant properties in vitro. Lastly, TIG1 expression correlated positively with Axl expression in primary human IBC specimens. Our findings establish that TIG1 positively modifies the malignant properties of IBC by supporting Axl function,

Corresponding Author: Naoto T. Ueno, Department of Breast Medical Oncology, Unit 1354, The University of Texas MD Anderson Cancer Center, 1515 Holcombe Blvd., Houston, TX 77030, USA. Phone: 713-792-8754; Fax: 713-794-4385; nueno@mdanderson.org.

Disclosure of Potential Conflicts of Interest:
No potential conflicts of interest were disclosed.

advancing understanding of its development and rationalizing TIG1 and Axl as promising therapeutic targets in IBC treatment.

Keywords

inflammatory breast cancer; tazarotene-induced gene 1; receptor tyrosine kinase Axl; tumorigenicity; migration; invasion

Introduction

Inflammatory breast cancer (IBC) is the most lethal and aggressive form of breast cancer (1). Despite progress in combined-modality treatment (chemotherapy, surgery, and radiation therapy), the long-term outcome of patients with IBC remains poor (2). IBC is also associated with a high risk of developing distant metastases, which is related to the lower survival rate of patients with IBC (3).

Efforts to unravel the molecular mechanism for the tumorigenicity and metastasis of IBC have yielded some successes such as the identification of several molecular changes, including loss of WISP3 and overexpression of Rho GTPase (4), E-cadherin (5), angiogenic factors (6), and translation initiation factor eIF4GI (7). Our previous results indicated that the EGFR pathway is involved in tumor growth and metastasis of IBC (8). A recent study showed that the metastatic, aggressive behavior of IBC may be mediated by a cancer stem cell component that displays aldehyde dehydrogenase 1 enzymatic activity (9). Although these findings have improved our understanding of IBC, the molecular mechanism underlying the aggressiveness of IBC is not well understood, and effective targeted therapies for this disease remain limited.

Tazarotene-induced gene 1 (*TIG1*), also known as *retinoic acid receptor responder 1*, is one of the genes highly upregulated in skin raft cultures by tazarotene (10), a synthetic retinoid. TIG1 protein contains a single membrane-spanning hydrophobic region and has been predicted to be a transmembrane protein. TIG1 resembles CD38, a retinoid-responsive molecule in immune cells, and might be structurally related to and analogous in function to CD38 (11). The expression of TIG1 in many tumor tissues and cell lines—including prostate cancer (12), endometrial cancer (13), and head and neck cancer (14)—is lost or silenced by hypermethylation of its promoter. TIG1 has been reported to be a potential tumor suppressor gene in human prostate cancer and endometrial cancer (12, 13).

The function of TIG1 in breast cancer is unknown. Recently, we identified *TIG1* as a potentially druggable gene that is highly expressed in triple-negative breast cancer and IBC in particular. By analyzing *TIG1* gene expression in patients with IBC and TNM-stage-matched non-IBC (15) and 3 independent non-IBC prognostic data sets (WANG (16), TRANSBIG (17), and MAINZ (18)), we found that in both IBC and non-IBC data sets, triple-negative breast cancer samples had significantly higher expression of TIG1 than did other clinical subtypes (estrogen receptor-positive/HER2-negative a nd HER2-positive). These findings raised the possibility that TIG1 may contribute to the aggressiveness of IBC, which drove us to investigate the role of TIG1 in the pathogenesis of IBC. In the study

reported here, we demonstrated that TIG1 correlates with shorter survival of patients with IBC and promotes tumor growth and invasion of IBC cells. We also identified the receptor tyrosine kinase Axl as a functional partner of TIG1 in IBC cells and revealed a mechanism that links TIG1 to the *Axl* gene in IBC.

Materials and Methods

Cell lines, reagents, and antibodies

SUM149 human IBC cells were purchased from Asterand (Detroit, MI). KPL-4 IBC cells were a kind gift from Dr. Junichi Kurebayashi (Kawasaki Medical School, Kawasaki, Japan). SUM149 and KPL-4 cells were validated using a short tandem repeat method based on primer extension to detect single base deviations in October 2010 and July 2013, respectively, by the Characterized Cell Line Core Facility at MD Anderson Cancer Center. SUM149 cells were cultured in Ham's F-12 medium supplemented with 5% fetal bovine serum (FBS) (Life Technologies, Inc.), 5 μg/mL insulin, and 1 μg/mL hydrocortisone. KPL-4 cells were grown in DMEM/F-12 medium supplemented with 10% FBS. The following primary antibodies were used: anti-TIG1 (R&D Systems), anti-Axl, anti-β-actin or -α-tubulin (Sigma-Aldrich Chemical Co.), anti-phospho-Axl (Tyr702) and anti-MMP-9 (Cell Signaling Technology), anti-Myc (Roche), anti-PCNA (Abcam), anti-lamin B (Calbiochem), anti-p65, anti-TIG1 (sc-98965), and anti-Axl (sc-20741) (Santa Cruz Biotechnology). The secondary fluorescent antibodies for Western blotting and immunofluorescence were from Molecular Probes and Invitrogen, respectively. Axl inhibitor SGI-7079 was provided by Tolero Pharmaceuticals, Inc.

All transfections were performed with FuGENE HD transfection reagent (Roche) following the manufacturer's guidelines.

Immunohistochemical staining and evaluation

Tissues from 88 patients with primary IBC who were treated at The University of Texas MD Anderson Cancer Center from September 1994 to August 2004 were included in this study. This study was approved by the MD Anderson Cancer Center Institutional Review Board. IHC staining was performed as described previously (19). An evaluation of the IHC results is described in detail in the Supplementary Materials and Methods.

Xenograft studies

Animal care and use were in accordance with institutional and NIH guidelines. The xenograft mouse model is described in the Supplementary Materials and Methods.

Proliferation, BrdU incorporation, migration, and invasion assays, anchorage-independent growth, and cell cycle analysis

These assays are described in detail in the Supplementary Materials and Methods.

DNA microarray analysis

siRNA transfection, RNA isolation, cDNA microarray, gene expression analysis, and statistical analysis were performed as described in the Supplementary Materials and

Methods. The microarray dataset has been deposited in the NCBI Gene Expression Omnibus database (http://www.ncbi.nlm.nih.gov/geo) with the accession number GSE30543.

Immunoblotting, immunoprecipitation, and cellular fractionation

These assays were performed as described in the Supplementary Materials and Methods.

Quantitative RT-PCR

Total RNA was extracted and purified using an RNeasy mini kit (Qiagen, Inc.) according to the manufacturer's instructions. The quantitative RT-PCR reactions were performed using an iScript One-Step RT-PCR kit with SYBR Green (Bio-Rad). Human β-actin mRNA was used as a normalization control. Primer sequences for TIG1, Axl, and β-actin are described in the Supplementary Materials and Methods.

Confocal microscopy and immunofluorescence assay

These assays are described in detail in the Supplementary Materials and Methods.

Statistical analysis

The 2-sided unpaired Student's *t* test was used for comparison between groups. Statistical analysis of the correlation between TIG1 expression and IBC patient survival (months) was performed using the 2-tailed unpaired Student's *t* test. The correlation between TIG1 and Axl expression in IBC tissues was performed by using Spearman's rank correlation coefficient. $P < 0.05$ was considered statistically significant.

Results

TIG1 is associated with shorter median survival in IBC patients

To assess the role of TIG1 in IBC pathogenesis and progression, we investigated TIG1 expression in 3 IBC cell lines—SUM149 (ER-negative/HER2-negative) (20), KPL-4 (ER-negative/HER2-positive) (21), and SUM190 (ER-negative/HER2-positive) (20)—and in IBC patient tissues. Our data showed that TIG1 was highly expressed in 2 of the 3 IBC cell lines, SUM149 and KPL-4, but not in IBC cell line SUM190, the non-IBC cell lines, or normal human mammary epithelial cell line MCF-10A (Fig. 1A). No staining of TIG1 was observed in normal breast tissues; however, the majority of IBC cases (56 of 76 cases, 73.7%) were TIG1-positive with high staining intensity (Fig. 1B). We observed a significant association between high TIG1 expression and a relatively worse clinical outcome in these IBC patients who had had preoperative chemotherapy (Fig. 1C, unpaired *t* test; $P = 0.0369$). There were no significant associations between TIG1 expression and other important clinicopathologic factors, such as age at diagnosis, lymph node status, histologic type, lymphovascular invasion, ER status, PR status, and HER2 status (Supplementary Table S1). Taken together, the high expression of TIG1 in human IBC patient tissues and cell lines and its positive correlation with poor clinical outcome of IBC patients indicated that TIG1 may contribute to the aggressiveness of IBC.

Silencing endogenous TIG1 reduces proliferation of IBC cells *in vitro* and inhibits tumor growth in a xenograft model

To investigate the role of TIG1 in IBC progression, we first assessed the effect of TIG1 silencing on IBC cell proliferation. Proliferation of SUM149 TIG1 stable knockdown clones shTIG1-A and shTIG1-D was decreased by 38% ($P < 0.001$) and 25% ($P = 0.001$), respectively, compared with proliferation of shControl cells (Fig. 2A and B). Time-course cell proliferation assays confirmed the reduced proliferation of shTIG1-A and shTIG1-D cells when grown for 48 and 72 hours (Supplementary Fig. S1A and S1B). BrdU incorporation in TIG1-depleted shTIG1-A and shTIG1-D cells was decreased by 18.4% and 14.7%, respectively, compared to that in shControl cells (Supplementary Fig. S1C). Decreased cell proliferation was observed in TIG1-knockdown KPL-4 cells (Supplementary Fig. S2A and S2B). We next evaluated the effect of TIG1 depletion on tumor growth in a SUM149 xenograft model (8). Injection of shTIG1-A or shTIG1-D cells resulted in much smaller tumors than did injection of SUM149 or shControl cells. On day 45, the mean tumor size from injection of shTIG1-A or shTIG1-D cells was 86% or 80%, respectively, smaller than the mean tumor size from injection of SUM149 cells ($P < 0.001$) (Fig. 2C). Immunoblotting analysis and immunofluorescence staining confirmed the depletion of TIG1 in shTIG1-A and shTIG1-D tumors (Fig. 2D and E), indicating that the reduction in tumor size was associated with depletion of TIG1. We also observed reduced expressions of proliferation marker PCNA in tumor tissues from injection of shTIG1-A or shTIG1-D cells (Fig. 2E). Taken together, silencing endogenous TIG1 reduced *in vitro* proliferation of IBC cells and inhibited tumor growth in an IBC xenograft model.

Silencing endogenous TIG1 reduces migration and invasion of IBC cells *in vitro*

Because patients with IBC are at high risk of recurrence in the form of metastatic disease, we investigated the effect of TIG1 knockdown on cell migration and invasion. Compared with migration and invasion of shControl cells, migration and invasion of shTIG1-A cells were reduced by 41% ($P < 0.001$) and 49% ($P < 0.001$), respectively, and migration and invasion of shTIG1-D cells were reduced by 39% ($P < 0.001$) and 48% ($P < 0.001$), respectively (Fig. 2F and G). We compared cell growth rates and found that TIG1 depletion did not cause a significant decrease in cell numbers within 24 hours (Supplementary Fig. S1A and S1B). Migration and invasion assays were performed within 6 and 18 hours, respectively, indicating that the slower rates of migration and invasion of TIG1-depleted cells were not caused by slower cell division. Similar results were observed in IBC KPL-4 cells (Supplementary Fig. S2C and S2D). To determine whether TIG1 knockdown affects the reorganization of the actin cytoskeleton, we used rhodamine-phalloidin to stain F-actin filaments in SUM149, shControl, and TIG1 knockdown cells. As shown in Fig. 2H, F-actin filaments were arranged into typical stress fibers in most of the parental or shControl cells. However, very few or no stress fibers were observed in the TIG1 knockdown cells; instead, phalloidin staining was diffusely distributed throughout the cytoplasm. Our data indicate that TIG1 knockdown in SUM149 cells impaired stress fiber formation. Moreover, TIG1-depleted shTIG1-A and shTIG1-D cells lost the ability to grow into Matrigel and showed an epithelial cell phenotype, which further supports the concept that TIG1 regulates the invasion of IBC cells (Supplementary Fig. S3). Taken together, these results indicated that silencing endogenous TIG1 reduced migration and invasion of IBC cells *in vitro*.

TIG1 restoration rescues the effects of TIG1 depletion cells

To further confirm the function of TIG1 in IBC cells, we restored TIG1 expression in TIG1-depleted shTIG1-A cells and found the proliferation of TIG1-restored pCMV6-TIG1 cells increased by 52.3% ($P < 0.005$), and their migration and invasion increased by 62.6% ($P < 0.001$) and 41.3% ($P = 0.001$), respectively, compared with shTIG1-A cells (Fig. 3A–3D). The rescue effect of TIG1 restoration confirmed the contribution of TIG1 to the proliferation and invasion of IBC cells.

Receptor tyrosine kinase Axl is a functional partner of TIG1

To investigate the underlying mechanism by which TIG1 promotes tumor growth and invasion of IBC cells, we compared gene expression profiles between SUM149 cells transfected with control siRNA and SUM149 cells transfected with siRNA targeting TIG1 using DNA microarray analysis. We selected as candidates 19 representative genes related to proliferation, migration, and invasion from 183 probe sets with at least two-fold change in expression ($P < 0.005$, 2-sample *t* test) (Supplementary Table S2 and Supplementary Fig. S4). We further validated the downregulation of one candidate, receptor tyrosine kinase Axl, in TIG1-depleted shTIG1-A and shTIG1-D cells at the mRNA (Fig. 4A, left panel) and protein levels (Fig. 4A, right panel, and Fig. 5B) and in tumors produced by injection of TIG1-depleted cells (Fig. 2E).

To test whether Axl is a potential functional partner of TIG1, we restored Axl expression in TIG1-depleted shTIG1-A cells and found it rescued the reduction in proliferation (19.0% rescued; $P < 0.005$), migration (87.4% rescued; $P < 0.001$), and invasion (79.1% rescued; $P < 0.001$) of shTIG1-A cells due to TIG1 silencing (Fig. 4B–4E and Supplementary Fig. S5A and S5B). Furthermore, depletion of Axl (shAxl-D and shAxl-E cells) has the same effects on the proliferation (38.5% reduced by shAxl-D [$P < 0.005$] and 48.8% reduced by shAxl-E [$P = 0.001$]), migration (32.7% reduced by shAxl-D [$P < 0.001$] and 31.7% reduced by shAxl-E [$P < 0.001$]), and invasion (36.7% reduced by shAxl-D [$P < 0.001$] and 39.8% reduced by shAxl-E [$P < 0.001$]) of SUM149 cells as those of TIG1 depletion (Fig. 4F–4I). Given that Axl restoration rescued the effects of TIG1 silencing and given that Axl depletion had the same effects as TIG1 depletion, we confirmed Axl as a potential functional partner of TIG1 in IBC cells.

We further examined the correlation between TIG1 and Axl expression in the same panel of IBC patient samples as shown in Fig. 1B and C. We found that TIG1 expression was positively correlated with Axl expression in IBC patient samples (Fig. 4J and Table 1, Spearman's rank correlation coefficient [$P < 0.005$]). Taken together, these data further suggest a link between TIG1 and Axl expression in the regulation of IBC progression.

TIG1 interacts with Axl and stabilizes Axl

To elucidate the link between TIG1 and Axl in the regulation of IBC progression, we first examined a possible interaction between TIG1 and Axl by reciprocal immunoprecipitation followed by immunoblotting analysis. Our results showed that endogenous TIG1 was specifically associated with Axl *in vivo* (Fig. 5A). We further detected the colocalization of TIG1 with Axl in SUM149 cells transfected with control shRNA but not with shRNA

targeting TIG1 (Fig. 5B). We also detected colocalization of TIG1 with Axl in KPL-4 cells (Supplementary Fig. S6). We further found that cotransfection of the pCMV6-TIG1 vector with the pCMV6-Axl vector in 293T cells increased the expression of Axl in a dose-dependent manner (Fig. 5C). Degradation of Axl has been proven to be metalloproteinase- and proteasome-dependent (22). Treatment with the proteasome inhibitor MG-132 fully restored Axl expression in TIG1-depleted shTIG1-A and shTIG1-D cells (Fig. 5D), indicating that TIG1 can stabilize Axl protein *in vivo* by inhibiting its proteasome-dependent degradation.

TIG1 regulates invasion of IBC cells through the Axl signaling pathway

Enhanced expression of MMP-9 is required for Axl-mediated invasion both *in vitro* and *in vivo*, and NF-κB signaling is found to be involved in Axl-enhanced MMP-9 activation (23). As shown in Fig. 5E, the MMP-9 level in TIG1-silenced clones shTIG1-A and shTIG1-D were significantly lower than were those in parental SUM149 or shControl cells. We also found that the nuclear accumulation of p65, an indicator of activation of NF-κB regulation, was significantly abolished in TIG1-depleted shTIG1-A and shTIG1-D cells (Fig. 5F). Taken together, the impact of TIG1 depletion on downstream molecules MMP-9 and NF-κB of the Axl signaling pathway suggests that TIG1 may regulate the invasion of IBC cells through the Axl signaling pathway.

Inhibition of the Axl signaling pathway reduces proliferation, migration, and invasion of IBC cells

To investigate the clinical relevance of our findings, we tested the effects of an Axl inhibitor, SGI-7079 (24), in IBC cells. SGI-7079 treatment inhibited the phosphorylation of Axl at Tyr 702 upon Gas 6 stimulation in SUM149 cells (Fig. 6A). SGI-7079 significantly inhibited the proliferation of SUM149 or KPL-4 cells with an IC_{50} of 0.43 μM or 0.16 μM, respectively, and induced sub-G1 cell cycle arrest (Fig. 6B and C). The growth of SUM149 and KPL-4 in soft agar, one of the hallmark characteristics of cellular transformation and uncontrolled cell growth, was also significantly inhibited by SGI-7079 treatment (Fig. 6D). SGI-7079 treatment also significantly decreased the migration and invasion of SUM149 cells (Fig. 6E) and the invasion of KPL-4 cells (Supplementary Fig. S7). Taken together, Axl inhibitor SGI-7079 significantly inhibited the proliferation, migration, and invasion of IBC cells, suggesting that Axl may be a promising therapeutic target in patients with IBC.

Discussion

In this study, we determined the contribution of a novel oncogenic gene, *TIG1*, to tumor growth and invasion of IBC cells. The capacity to migrate and invade through tissue barriers is essential for cancer cells to complete the process of metastasis (25). The contribution of TIG1 to the invasion of IBC suggests that TIG1 might play a role in metastasis. The tumorigenic and potential metastatic function of TIG1 revealed in our study may be cancer-type specific. Previous reports showed that TIG1 is a tumor suppressor in other cancer types, such as prostate cancer and endometrial cancer (12, 13). In contrast with those reports, we observed high expression frequency of TIG1 protein in IBC specimens and cell lines and

noted the inhibitory effects of TIG1 depletion on cell proliferation and tumor growth of IBC. These results indicate that TIG1 contributes to tumor growth of IBC.

The most important finding in our study was the statistically significant correlation between high TIG1 expression and poorer patient median survival seen in the box-and-whisker plot. Ideally, we would have confirmed this correlation using other standard plotting methods, such as the widely used Kaplan-Meier method. However, our small patient sample size (88 samples) and the censoring of some survival data in our sample rendered these methods less informative than they would be in a larger population. Using the box-and-whisker plot as an exploratory method, however, we demonstrated a correlation between TIG1 expression (after chemotherapy) and IBC patient median survival duration, which suggests the contribution of TIG1 to the malignant process of IBC and the importance of determining whether TIG1 serves as a prognostic marker for IBC patients using preoperative chemotherapy samples in a future investigation.

Among the other interesting findings in this study were the identification of a linkage between TIG1 and the Axl signaling pathway, a critical element in the signaling network regulating migration and invasion of breast cancer cells. Our results indicated that TIG1 stabilizes Axl by inhibiting the proteasome-dependent degradation of Axl. TIG1 depletion downregulates Axl expression and inactivates NF-κB, which leads to downregulation of MMP-9, ultimately leading to decreased invasion of IBC cells. These results suggest that TIG1 regulates the invasion of IBC cells through mediation of the Axl signaling pathway. The positive correlation between TIG1 and Axl expression in IBC patient samples revealed in our study further supports the importance of TIG1 and Axl linkage in the regulation of IBC progression. To our knowledge, this is the first report to describe the mechanism by which TIG1 promotes invasion of IBC cells and the signaling pathway that TIG1 participates in.

The identification of Axl as a functional partner of TIG1 suggests that Axl might be a potential target for therapeutic intervention in IBC. Thus, blocking the Axl signaling pathway may inhibit the growth and invasion of IBC cells. Indeed, our data demonstrated that depleting Axl with use of shRNA and inhibiting the tyrosine kinase activity of Axl with use of the small molecule inhibitor SGI-7079 significantly decreased the proliferation, migration, and invasion of IBC cells, suggesting that Axl is a promising therapeutic target in patients with IBC. Moreover, the tumorigenic function of TIG1 revealed in this study suggests that TIG1 might be an attractive therapeutic target for the treatment of IBC, which will be investigated in future studies by delivering neutral liposome (DOPC)-encapsulated TIG1 siRNA to tumors to determine whether it can inhibit tumor growth in an IBC xenograft model.

In summary, our findings show that TIG1 plays an important role in the pathogenesis of IBC by promoting tumor growth and invasion through the oncogenic gene *Axl* and furthermore, that TIG1 and Axl are promising therapeutic targets in patients with IBC.

Supplementary Material

Refer to Web version on PubMed Central for supplementary material.

Acknowledgments

We thank Sunita C. Patterson, Stephanie P. Deming, and Tamara K. Locke of the Department of Scientific Publications at The University of Texas MD Anderson Cancer Center for their expert editorial assistance. We thank Dr. Nianxiang Zhang, Dr. Keith Baggerly, and the Genomics Core Facility at MD Anderson Cancer Center for cDNA microarray analysis. STR DNA fingerprinting was done by the Cancer Center Support Grant-funded Characterized Cell Line core, NCI # CA016672. We thank Dr. Shengyu Yang of the Department of Tumor Biology at the H. Lee Moffitt Cancer Center and Research Institute for his assistance with the actin cytoskeleton analysis. We thank Dr. Yi Du and Dr. Zhenbo Han of MD Anderson's Department of Molecular and Cellular Oncology for their assistance with the microscopy analysis.

Grant Support

This work was supported by NIH grant R01 CA123318 (NT Ueno), The State of Texas Grant for Rare and Aggressive Cancers through the Morgan Welch Inflammatory Breast Cancer Research Program (NT Ueno), and NIH Cancer Center Support Grant CA016672.

References

1. Cristofanilli M, Buzdar AU, Hortobagyi GN. Update on the management of inflammatory breast cancer. Oncologist 2003;8:141–8. [PubMed: 12697939]
2. Gonzalez-Angulo AM, Hennessy BT, Broglio K, Meric-Bernstam F, Cristofanilli M, Giordano SH, et al. Trends for inflammatory breast cancer: is survival improving? Oncologist 2007;12:904–12. [PubMed: 17766649]
3. Jaiyesimi IA, Buzdar AU, Hortobagyi G. Inflammatory breast cancer: a review. J Clin Oncol 1992;10:1014–24. [PubMed: 1588366]
4. van Golen KL, Davies S, Wu ZF, Wang Y, Bucana CD, Root H, et al. A novel putative low-affinity insulin-like growth factor-binding protein, LIBC (lost in inflammatory breast cancer), and RhoC GTPase correlate with the inflammatory breast cancer phenotype. Clin Cancer Res 1999;5:2511–9. [PubMed: 10499627]
5. Alpaugh ML, Tomlinson JS, Ye Y, Barsky SH. Relationship of sialyl-Lewis(x/a) underexpression and E-cadherin overexpression in the lymphovascular embolus of inflammatory breast carcinoma. Am J Pathol 2002;161:619–28. [PubMed: 12163386]
6. Van der Auwera I, Van Laere SJ, Van den Eynden GG, Benoy I, van Dam P, Colpaert CG, et al. Increased angiogenesis and lymphangiogenesis in inflammatory versus noninflammatory breast cancer by real-time reverse transcriptase-PCR gene expression quantification. Clin Cancer Res 2004;10:7965–71. [PubMed: 15585631]
7. Silvera D, Arju R, Darvishian F, Levine PH, Zolfaghari L, Goldberg J, et al. Essential role for eIF4GI overexpression in the pathogenesis of inflammatory breast cancer. Nat Cell Biol 2009;11:903–8. [PubMed: 19525934]
8. Zhang D, LaFortune TA, Krishnamurthy S, Esteva FJ, Cristofanilli M, Liu P, et al. Epidermal growth factor receptor tyrosine kinase inhibitor reverses mesenchymal to epithelial phenotype and inhibits metastasis in inflammatory breast cancer. Clin Cancer Res 2009;15:6639–48. [PubMed: 19825949]
9. Charafe-Jauffret E, Ginestier C, Iovino F, Tarpin C, Diebel M, Esterni B, et al. Aldehyde dehydrogenase 1-positive cancer stem cells mediate metastasis and poor clinical outcome in inflammatory breast cancer. Clin Cancer Res16:45–55. [PubMed: 20028757]
10. Nagpal S, Patel S, Asano AT, Johnson AT, Duvic M, Chandraratna RA. Tazarotene-induced gene 1 (TIG1), a novel retinoic acid receptor-responsive gene in skin. J Invest Dermatol 1996;106:269–74. [PubMed: 8601727]
11. Nagpal S, Chandraratna RA. Recent developments in receptor-selective retinoids. Curr Pharm Des 2000;6:919–31. [PubMed: 10828316]

12. Jing C, El-Ghany MA, Beesley C, Foster CS, Rudland PS, Smith P, et al. Tazarotene-induced gene 1 (TIG1) expression in prostate carcinomas and its relationship to tumorigenicity. J Natl Cancer Inst 2002;94:482–90. [PubMed: 11929948]
13. Takai N, Kawamata N, Walsh CS, Gery S, Desmond JC, Whittaker S, et al. Discovery of epigenetically masked tumor suppressor genes in endometrial cancer. Mol Cancer Res 2005;3:261–9. [PubMed: 15886297]
14. Tokumaru Y, Yahata Y, Fujii M. Aberrant promoter hypermethylation of tazarotine-induced gene 1 (TIG1) in head and neck cancer. Nippon Jibiinkoka Gakkai Kaiho 2005;108:1152–7. [PubMed: 16440812]
15. Iwamoto T, Bianchini G, Qi Y, Cristofanilli M, Lucci A, Woodward WA, et al. Different gene expressions are associated with the different molecular subtypes of inflammatory breast cancer. Breast Cancer Res Treat 2011;125:785–95. [PubMed: 21153052]
16. Wang Y, Klijn JG, Zhang Y, Sieuwerts AM, Look MP, Yang F, et al. Gene-expression profiles to predict distant metastasis of lymph-node-negative primary breast cancer. Lancet 2005;365:671–9. [PubMed: 15721472]
17. Buyse M, Loi S, van't Veer L, Viale G, Delorenzi M, Glas AM, et al. Validation and clinical utility of a 70-gene prognostic signature for women with node-negative breast cancer. J Natl Cancer Inst 2006;98:1183–92. [PubMed: 16954471]
18. Schmidt M, Bohm D, von Torne C, Steiner E, Puhl A, Pilch H, et al. The humoral immune system has a key prognostic impact in node-negative breast cancer. Cancer Res 2008;68:5405–13. [PubMed: 18593943]
19. Deng J, Miller SA, Wang HY, Xia W, Wen Y, Zhou BP, et al. Beta-catenin interacts with and inhibits NF-kappa B in human colon and breast cancer. Cancer Cell 2002;2:323–34. [PubMed: 12398896]
20. Grigoriadis A, Mackay A, Noel E, Wu PJ, Natrajan R, Frankum J, et al. Molecular characterisation of cell line models for triple-negative breast cancers. BMC Genomics 2012;13:619. [PubMed: 23151021]
21. Robertson FMCK, Fernandez SV, Zh Mu, Zhang X, Liu H, et al. Genomic profiling of pre-clinical models of inflammatory breast cancer identifies a signature of epithelial plasticity and suppression of TGFβ signaling. J Clin Exp Pathol 2012;2:1–11.
22. Wilhelm I, Nagyoszi P, Farkas AE, Couraud PO, Romero IA, Weksler B, et al. Hyperosmotic stress induces Axl activation and cleavage in cerebral endothelial cells. J Neurochem 2008;107:116–26. [PubMed: 18673450]
23. Tai KY, Shieh YS, Lee CS, Shiah SG, Wu CW. Axl promotes cell invasion by inducing MMP-9 activity through activation of NF-kappaB and Brg-1. Oncogene 2008;27:4044–55. [PubMed: 18345028]
24. Byers LA, Diao L, Wang J, Saintigny P, Girard L, Peyton M, et al. An epithelial-mesenchymal transition gene signature predicts resistance to EGFR and PI3K inhibitors and identifies Axl as a therapeutic target for overcoming EGFR inhibitor resistance. Clin Cancer Res 2013;19:279–90. [PubMed: 23091115]
25. Steeg PS. Tumor metastasis: mechanistic insights and clinical challenges. Nat Med 2006;12:895–904. [PubMed: 16892035]

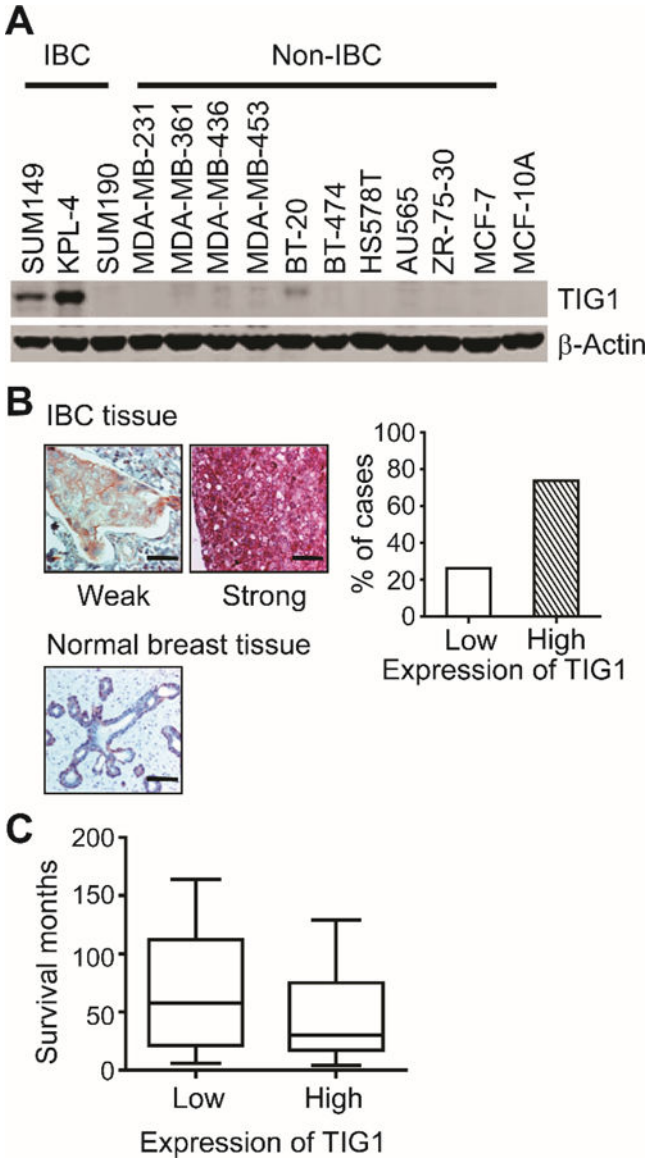

Figure 1.

TIG1 is highly expressed in human inflammatory breast cancer (IBC) tissues and cell lines and correlates with poor median survival of IBC patients. A, The expression of TIG1 was tested with Western blotting in 3 IBC cell lines, 10 non-IBC cell lines, and a normal human mammary epithelial cell line (MCF-10A). B, Representative immunohistochemical staining of TIG1 protein in IBC tissues (top panel) and normal breast tissue (bottom panel). Scale bars: 50 μm. Quantitative results are shown in right panel. C, Box plot of survival (months) of IBC patients with high or low TIG1 expression. Boxes include values in the 25%−75% interval; central lines represent the median value; whiskers show the lowest and highest values. $P = 0.0369$.

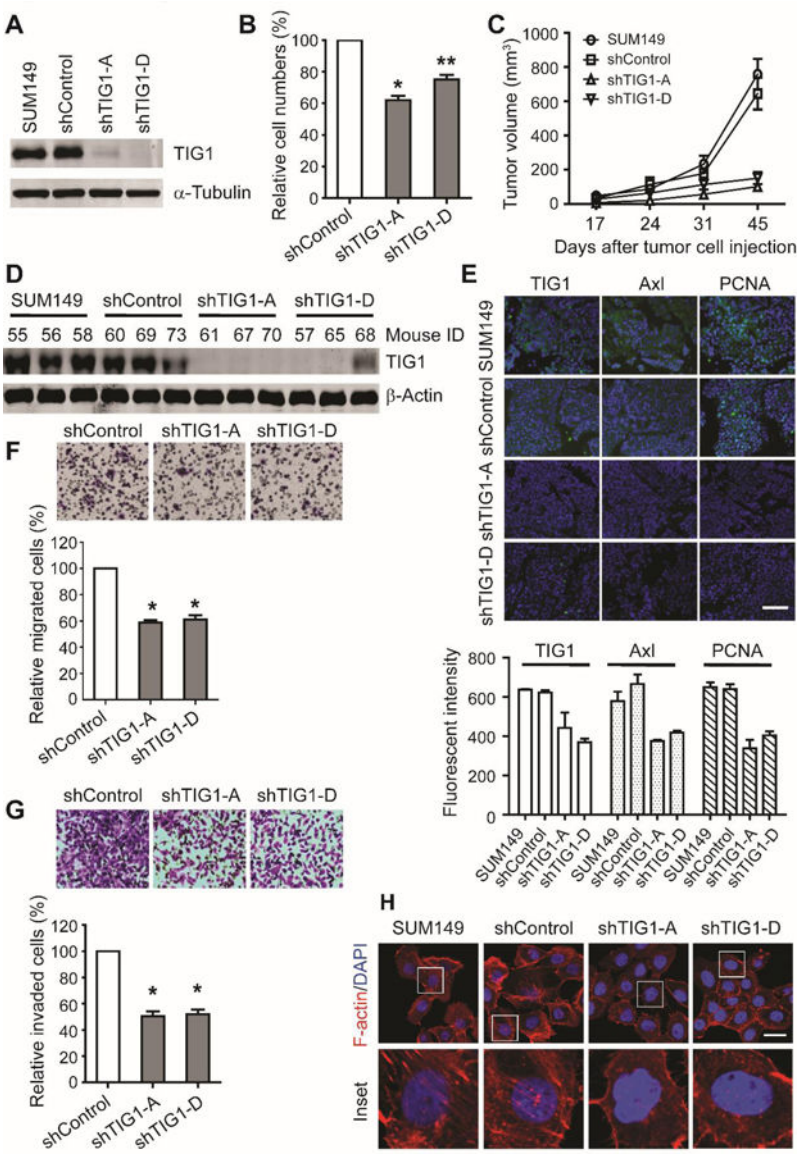

Figure 2.

Silencing endogenous TIG1 in SUM149 IBC cells inhibits cell proliferation, migration, invasion *in vitro* and inhibits tumor growth in a xenograft model. A, SUM149 cells were transfected with control (shControl) or TIG1-targeted (shTIG1-A and shTIG1-D) shRNAs. Expression of TIG1 in parental SUM149 cells and in the stable clones shControl, shTIG1-A, and shTIG1-D was analyzed by Western blotting. B, Proliferation of TIG1 shRNA knockdown cells was compared with that of control shRNA knockdown cells by using the trypan blue exclusion assay. Experiments were independently repeated 3 times. Bars, ± SDs. * $P < 0.001$, ** $P = 0.001$. C, Tumor growth of TIG1 knockdown shTIG1-A and shTIG1-D cells was compared with that of SUM149 and shControl cells. For comparison of day 45 tumor volume between mice injected with shTIG1-A or shTIG1-D cells and those injected with SUM149 cells, the P value was < 0.001. Bars, ± SDs. D, Expressions of TIG1 in tumor samples from each mouse were analyzed with Western blotting. E, Representative images of

immunofluorescence staining of tumor tissues with TIG1, Axl, and PCNA antibodies. Scale bar: 200 μm. The relative fluorescence intensity from the images is shown in the bottom panel. Bars, ± SDs. F, shRNA-transfected SUM149 cells were analyzed for transwell migration by crystal violet staining (top panel); quantitative results are shown in the bottom panel. Experiments were independently repeated 3 times. Bars, ± SDs. * $P < 0.001$. G, shRNA-transfected SUM149 cells were analyzed for invasion through Matrigel by crystal violet staining (top panel); quantitative results are shown in the bottom panel. Experiments were independently repeated 3 times. Bars, ± SDs. * $P < 0.001$. H, SUM149 and shRNA-transfected SUM149 cells were analyzed for actin organization by immunofluorescence analysis using rhodamine-phalloidin (F-actin, red). Nuclei were labeled with DAPI (blue). Scale bar: 10 μm.

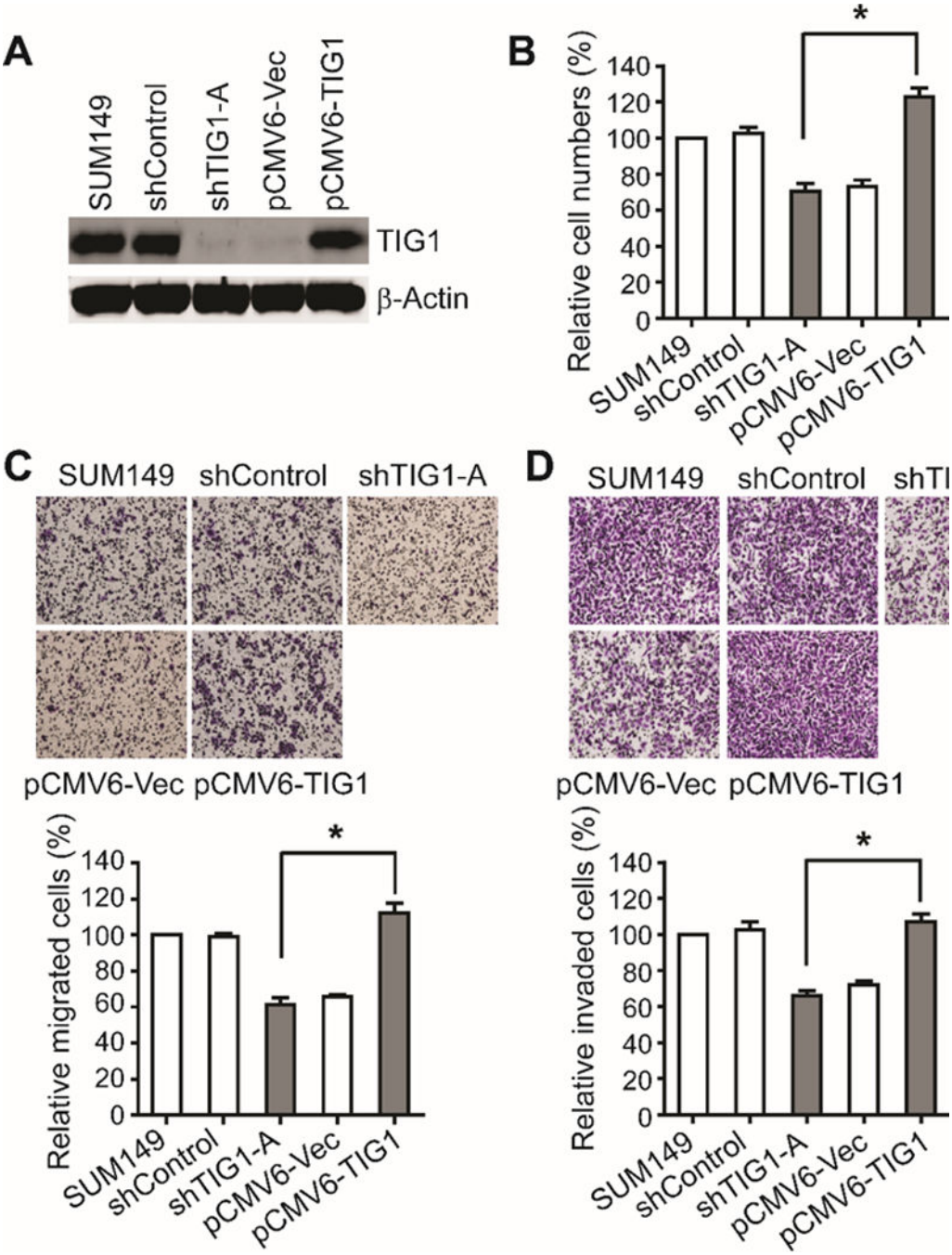

Figure 3.

Restoration of TIG1 expression rescues the proliferation, migration, and invasion of shTIG1-A cells. A, Control vector pCMV6-Vec or TIG1 expression vector pCMV6-TIG1 was transfected into TIG1-silenced shTIG1-A cells. Stable clones (pCMV6-Vec and pCMV6-TIG1) were selected with puromycin and neomycin. The restoration of TIG1 was analyzed by Western blotting. B, Proliferation of the cells in (A) was measured by counting viable cells using the trypan blue exclusion assay. Bars, ± SDs. * $P < 0.005$. C, The cells in (A) were analyzed for transwell migration by crystal violet staining (top panel); quantitative

results are shown in the bottom panel. Bars, ± SDs. * $P < 0.001$. D, The cells in (A) were analyzed for Matrigel invasion by crystal violet staining (top panel); quantitative results are shown in the bottom panel. Bars, ± SDs. * $P = 0.001$. Experiments in B, C, and D were independently repeated 3 times.

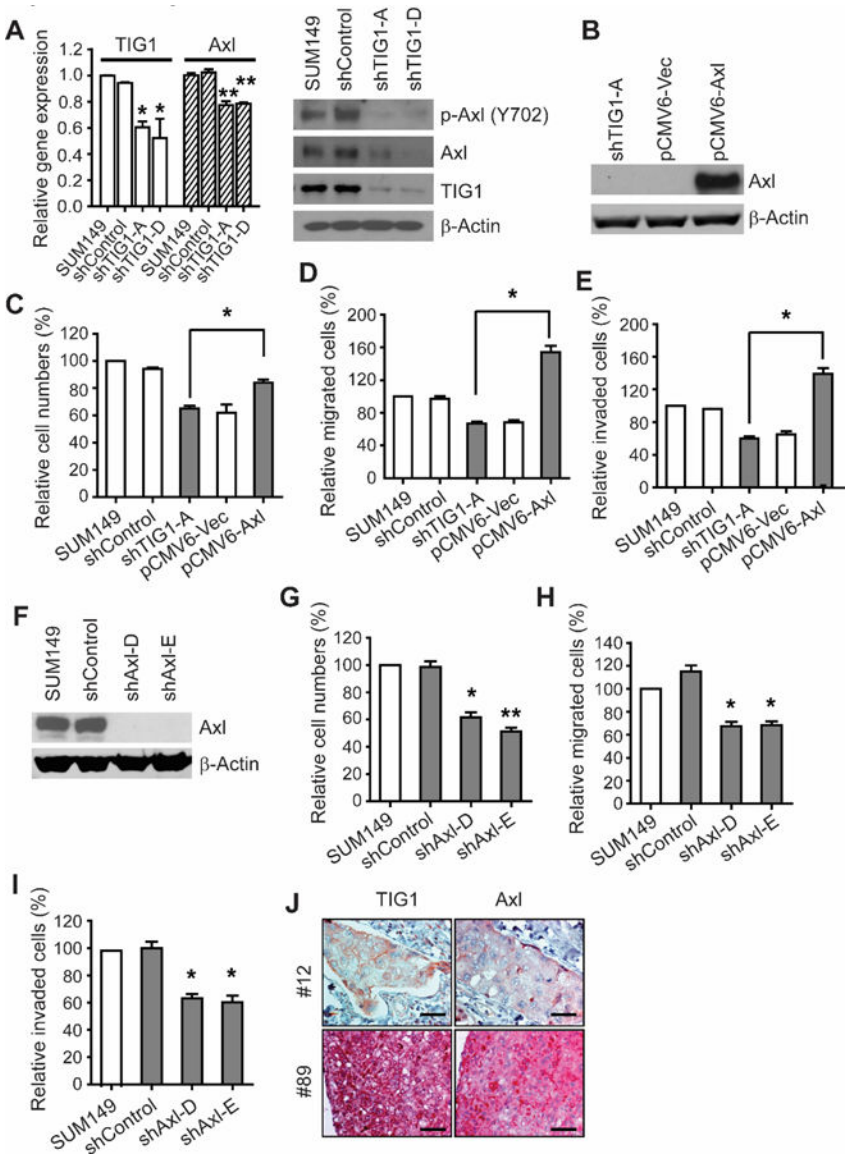

Figure 4.

Axl is a potential functional partner of TIG1 in IBC cells. A, The expression of Axl was compared between TIG1-depleted cells (shTIG1-A and shTIG1-D), parental SUM149 cells, and shControl cells by using qRT-PCR (left panel) and Western blotting (right panel). Bars, ± SDs. * $P < 0.01$; ** $P < 0.001$. B, Control vector pCMV6-Vec or Axl expression vector pCMV6-Axl was transiently transfected into TIG1-silenced shTIG1-A cells. The restoration of Axl was analyzed with Western blotting by examining the expression of Axl in the indicated cells after transfection for 72 hours. C, Proliferation of the cells in (B) was measured by counting viable cells using the trypan blue exclusion assay. Bars, ± SDs. * $P < 0.005$. D, The cells in (B) were analyzed for transwell migration. Bars, ± SDs. * $P < 0.001$. E, The cells in (B) were analyzed for Matrigel invasion. Bars, ± SDs. * $P < 0.001$. F, SUM149 cells were transfected with control (shControl) or Axl-targeted (shAxl-D and shAxl-E) lentiviral shRNAs. The knockdown of Axl was analyzed by Western blotting. G,

Proliferation of the cells in (F) was measured by counting viable cells using the trypan blue exclusion assay. Bars, ± SDs. * $P < 0.005$, ** $P = 0.001$. H, The cells in (F) were analyzed for transwell migration. Bars, ± SDs. * $P < 0.001$. I, The cells in (F) were analyzed for Matrigel invasion. Bars, ± SDs. * $P < 0.001$. J, Representative images of IHC staining for TIG1 (left panel) and Axl (right panel) protein in IBC tissues. #12 and #89 are patient ID numbers. Top: weak expression; bottom: strong expression. Scale bars: 50 μm. Experiments were repeated 3 times independently.

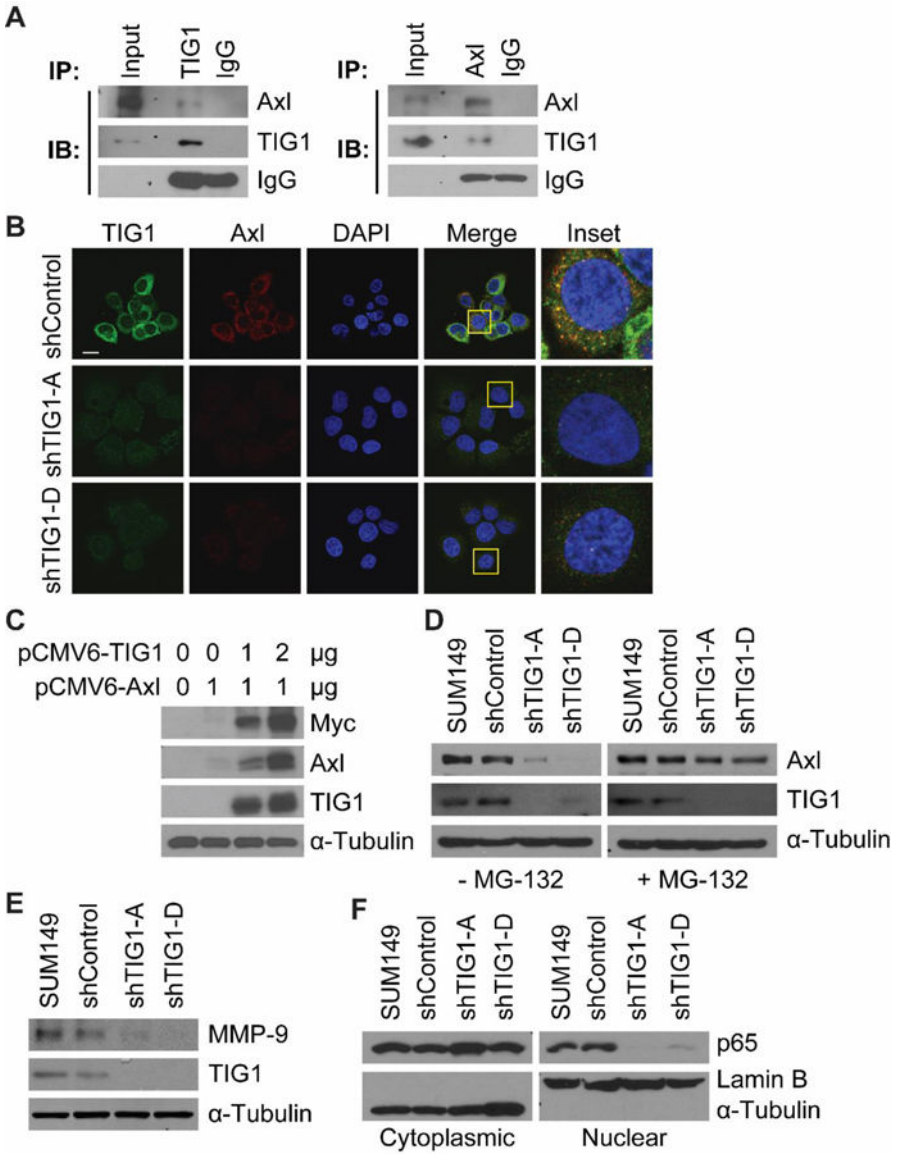

Figure 5.

TIG1 interacts with Axl and stabilizes Axl *in vivo* and regulates invasion of IBC cells through the Axl signaling pathway. A, Interaction between endogenous TIG1 and Axl in SUM149 cells was examined with immunoprecipitation by using anti-TIG1 antibody, followed by Western blotting using anti-Axl antibody (left panel). Reciprocal immunoprecipitation is shown in the right panel. B, TIG1 colocalized with Axl in SUM149 cells. The colocalization of TIG1 with Axl was examined with confocal microscopy. TIG1 and Axl were immunofluorescently stained as green and red, respectively. Nuclei were counterstained with DAPI (blue). Scale bars: 10 μm. The boxed areas are shown in insets. C, Ectopic expression of TIG1 increased the protein level of Axl. 293T cells were cotransfected with 1 μg of pCMV6-Axl plasmid plus different amounts of pCMV6-TIG1 plasmid. Then the expression level of Axl was examined with Western blotting by using anti-Axl and anti-Myc antibodies. D, Proteasome inhibitor MG-132 restored Axl expression in TIG1-depleted

cells. SUM149, shControl, shTIG1-A, and shTIG1-D cells were not treated or were treated with 10 μmol/L MG-132 for 6 hours and then harvested for Western blotting by using anti-Axl, anti-TIG1, and anti-tubulin antibodies. E, Expression of MMP-9 was compared between TIG1 knockdown cells (shTIG1-A and shTIG1-D), parental SUM149 cells, and shControl cells by using Western blotting. F, Silencing TIG1 decreased the nuclear translocation of p65 of NF-κB. The cytoplasmic and nuclear fractions of SUM149, shControl, shTIG1-A, and shTIG1-D cells were prepared, and the protein level of p65 in these fractions was examined with Western blotting. Lamin B and α-tubulin served as markers of nuclear and cytoplasmic fractions, respectively.

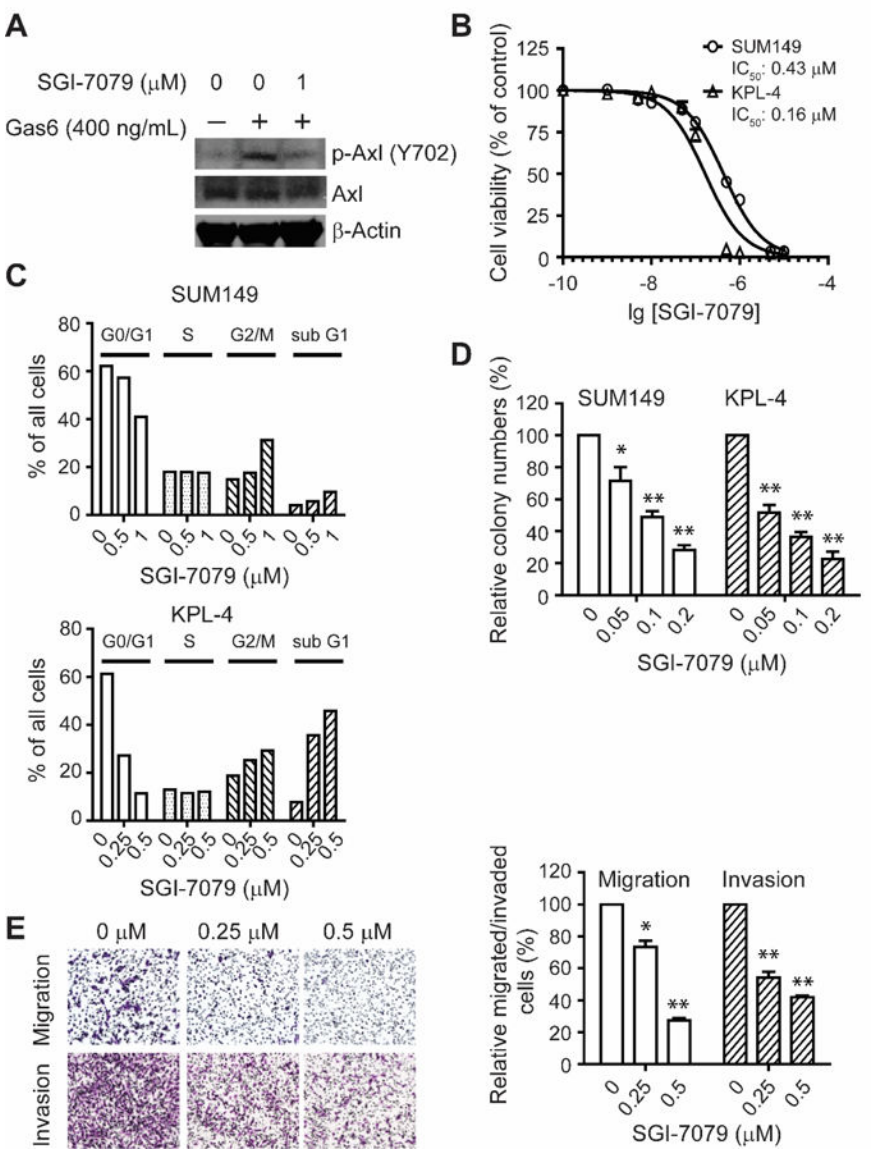

Figure 6.

Axl inhibitor SGI-7079 inhibited the proliferation, migration, and invasion of IBC cells. A, SGI-7079 inhibits the Axl signaling pathway in SUM149 cells. SUM149 cells were serum-starved overnight and treated with 0 (vehicle) and 1 μM SGI-7079 for 5 hours. The phosphorylation of Axl at Y702 upon Gas (400 ng/mL) stimulation for 20 min was analyzed by Western blotting. B, SUM149 inhibits the proliferation of SUM149 and KPL-4 cells. SGI-7079 IC_{50} in SUM149 and KPL-4 cells was measured after 72 hours of treatment using the CellTiter-Blue cell viability assay. IC_{50} in SUM149 and KPL-4 cells is 0.43 μM and 0.16 μM, respectively. C, SGI-7079 induces sub-G1 arrest in SUM149 and KPL-4 cells. SUM149 (top panel) and KPL-4 (bottom panel) cells were treated with SGI-7079 at indicated concentration for 48 hours, and FACScan analysis was performed to detect the cell cycle distribution. D, SGI-7079 treatment inhibits growth of SUM149 and KPL-4 cells in soft agar. SUM149 and KPL-4 cells were plated in soft agar with SGI-7079 at indicated

concentration. Colonies were stained with 4 mg/mL MTT for 1 hour and then counted with GelCount. Bars, ± SDs. * $P < 0.05$, ** $P < 0.001$. E, SGI-7079 treatment inhibits the migration and invasion of SUM149 cells. SUM149 cells were treated with SGI-7079 at indicated concentration and then subjected to transwell migration and invasion through Matrigel assays. Left panel: representative images of crystal violet staining. Right panel: quantitative results. Bars, ± SDs. * $P < 0.01$, ** $P < 0.001$. All experiments were repeated 3 times independently.

Table 1.

TIG1 expression positively correlates with Axl expression in IBC patient samples.

		TIG1 expression		
		Low	**High**	**Total**
Axl expression	Low	12 (17.4%)	9 (13.0%)	21 (30.4%)
	High	6 (8.7%)	42 (60.9%)	48 (69.6%)
Total		18 (26.1%)	51 (73.9%)	69 (100.0%)

Expression patterns of TIG1 and Axl in IBC patient samples were determined and summarized. The correlation between TIG1 and Axl was analyzed using Spearman's rank correlation coefficient ($P < 0.005$).